

2-19-92
E6608

NASA Technical Memorandum 105324
IEPC-91-076

Preliminary Test Results of a Hollow Cathode MPD Thruster

Maris A. Mantenieks
National Aeronautics and Space Administration
Lewis Research Center
Cleveland, Ohio

and

Roger M. Myers
Sverdrup Technology, Inc.
Lewis Research Center Group
Brook Park, Ohio

Prepared for the
22nd International Electric Propulsion Conference
cosponsored by the AIDAA, AIAA, DGLR, and JSASS
Viareggio, Italy, October 14-17, 1991



PRELIMINARY TEST RESULTS OF A HOLLOW CATHODE MPD THRUSTER

M.A. Mantenicks
National Aeronautics and Space Administration
Lewis Research Center
Cleveland, Ohio 44135

and

R.M. Myers
Sverdrup Technology, Inc.
Lewis Research Center Group
Brook Park, Ohio 44142

ABSTRACT

Performance of four hollow cathode configurations with low work function inserts has been evaluated in a steady-state 100 kW class applied magnetic field MPD thruster. Two of the configurations exhibited stable discharge current attachment to the low work function inserts of the hollow cathodes. A maximum discharge current of 2250 A was attained. While the applied-field increased the performance of the thruster, at high applied-fields the discharge current attachment moved from the insert to the cathode body. The first successful hollow cathode performed well in comparison with a conventional rod cathode MPD thruster, attaining a thrust efficiency with argon of close to 20 percent at a specific impulse of about 2000 s. The second successful configuration had significantly lower performance.

INTRODUCTION

Magnetoplasmadynamic (MPD) thruster systems have been proposed for applications involving Earth-orbit transfer and interplanetary missions. Recent interest in high power missions has reinvigorated both steady-state and quasi-steady MPD thruster research (ref. 1). Even though considerable effort was expended in MPD thruster technology in the 1960's and 1970's, thrust efficiency with propellants other than lithium was low, and electrode erosion generally precluded extended life demonstrations. Attention has recently been focused on applied magnetic field thrusters due to the potential for higher performance at power levels from 30 to 200 kW (ref. 2).

Significant progress has been recently made in cathode erosion rate measurement techniques, cathode diagnostics, and the understanding of MPD thruster cathode erosion processes. Measured cathode erosion rates range from about 5×10^{-4} to $0.2 \mu\text{g}/\text{C}$ for steady-state and quasi-steady thrusters, respectively (ref. 2). While cathode erosion rates have been reduced significantly by utilizing ultra-high purity propellants, the rates are still unacceptably high for most MPD thruster missions requiring several thousand hours of operation at discharge currents of several kiloamperes.

The surface temperature of a typical 2 percent thoriated tungsten MPD thruster cathode has been measured to be approximately 3000 °C, for which the principal cathode erosion mechanism was sublimation (refs. 3 to 5). The actual net erosion rate seemed to be governed by the relative magnitudes of sublimation and backscattering of the escaped atoms from the cathode surface, and was thus dependent on the ambient pressure at the cathode surface. The

decrease in erosion rates with increasing ambient pressure has been well documented for MPD and thermal arcjet thrusters (refs. 6 to 8).

The exponential dependence of the sublimation rate on surface temperature indicates the desirability of reducing the cathode operating temperature while maintaining the same current density. This can be accomplished by reducing the cathode work function. The resulting benefits have been convincingly demonstrated by experiments comparing operation with thoriated and pure tungsten cathodes (ref 8). Further improvements of cathode lifetime should result from using a cathode material with a lower work function and a cathode design in which the low work function material is not depleted during the required lifetime of the cathode.

The best demonstrated combination of low work function and long life has been offered by the hollow cathode with a barium impregnated tungsten insert (ref. 9). A schematic of such a device used in a MPD thruster is shown in figure 1. While the term "hollow cathode" has been applied to several electron emission configurations, the hollow cathode used in ion thrusters, as well as tests reported here, consisted of a refractory metal cathode body with a cylindrical porous tungsten insert impregnated with barium-calcium-aluminate compound with a molar fraction ratio of 4-1-1. The front of the cathode was enclosed by a disc with a centrally located orifice.

Recent testing with quasi-steady thrusters has demonstrated the benefits of barium impregnated cathodes. In these tests, the impregnated material reduced the erosion to the lowest rate measured in a quasi-steady thruster (ref. 10).

There are two central reasons to expect a longer life and improved thruster performance from a hollow cathode configuration. First, the orifice of the hollow cathode should increase the residence time of the sublimated barium atoms inside the cathode chamber. Second, the ability to control the propellant mass flow rate through the cathode should enable regulation of the ambient pressure at the cathode surface and thus reduce the loss of barium atoms due to sublimation. In addition, the performance of a MPD thruster with a hollow cathode may improve due to the decrease of the cathode fall voltage necessary to emit electrons.

Lanthanum hexaboride has also been used as a low work function cathode material in dense plasma production devices (ref. 11). However, hollow cathodes using barium impregnated inserts in ion thrusters have had the most successful and extensive track record. Ion thrusters with hollow cathodes have accumulated over 10 000 hr in thruster lifetests (refs. 9 and 12), and up to 37 000 hr in cathode component tests (ref. 13). Life tests of hollow cathodes in ion thrusters exhibited long lifetime because the insert temperature was relatively low, between 1000 and 1100 °C. In this temperature range, the depletion rate of low work function material is extremely small (ref. 9). Tests have indicated that hollow cathodes operate optimally in the pressure range of 0.5 to 2 KPa, at discharge currents of about 20 A (ref. 14). This may explain why attempts to apply them to arcjet type thrusters were unsuccessful.

There have been several attempts at using hollow cathodes without low work function inserts in quasi-steady MPD thrusters. Thruster performance with a tungsten tube cathode was better than that of a solid rod (ref. 15). Lower cathode erosion and improved performance was obtained with a thoriated tungsten hollow cathode (ref. 16). Extensive studies have been performed with hollow refractory tubes (refs. 17 and 18). Generally, cathodes without low work function inserts suffer high erosion rates. For hollow cathodes to be successfully incorporated in MPD thrusters, the emission current capability of the cathode will have to be increased from

tens of amperes, where present generation ion thrusters operate, to thousands of amperes. This paper describes the first attempt to incorporate a hollow cathode with a low work function insert into a steady-state MPD thruster. Four hollow cathode configurations were tested. For those configurations with which steady-state operation was achieved, the thruster performance was mapped and compared with thrusters with conventional rod-shaped cathodes. The paper is concluded with a discussion of possible cathode deterioration mechanisms during the 20 hr tests.

APPARATUS AND TEST PROCEDURE

The test facility consisted of a vacuum chamber, thrust stand, power system, a propellant metering panel, water cooling apparatus, data acquisition system, a conventional water cooled cylindrical MPD thruster anode, and four hollow cathode configurations. The following describes each component of the system.

MPD THRUSTER TEST FACILITY

The hollow cathode MPD thruster was tested in a 7.6 m diameter, 21 m long vacuum chamber. The thruster was mounted on a thrust stand inside a 3 m diameter test chamber separated from the main tank by a 3 m diameter gate valve. The main tank was pumped by twenty oil diffusion pumps, backed by three lobe-type blowers and two roughing pumps. The facility maintained a no-load pressure of 0.001 Pa and maintained a pressure below 0.07 Pa at argon flow rates below 0.16 g/sec or hydrogen flow rates below 0.03 g/sec. The MPD thruster test facility is described in more detail in references 19 and 20.

The thrust-stand, fully described in reference 21 and shown schematically in figure 2, was an inverted pendulum whose upright flexures were designed to deflect about 5 cm at a thrust of 5 N. Remote calibrations of the stand were obtained by applying small weights along the thrust axis. Tares due to thruster discharge current and applied magnetic field were less than 3 percent of measured thrust for discharge currents up to 2500 A and magnet currents up to 1000 A.

The power system was composed of six welding supplies in a series-parallel network, a high voltage arc igniter, a magnet power supply, and safety sensors and interlocks. The network, which supplied up to 3000 A at 130 V, was electrically isolated from ground. A single welding supply provided up to 1500 A to the applied-field magnet. The discharge igniter was a 2 kW, 900 V dc supply.

Propellant was fed to the thruster using two independent flow paths, as shown in figure 1. Independent flow control was provided through the hollow cathode and insulating backplate. The system also allowed mixing of two gases. Propellant flow rates were measured using thermal conductivity type flow controllers with 2 percent precision.

Water cooling to the arc and magnet was provided by separate pump/heat exchanger assemblies, capable of supplying 0.8 liter/sec of water at a pressure of 1 MPa. The MPD thruster cathode and anode were cooled by the same pump/heat exchanger using deionized water in the closed-loop system. Water flow rates were obtained from a calibrated turbine meter. The power lost to the electrodes was obtained by measuring the water flow rate and the change in water temperature. Digital readouts were used to indicate the water temperature to the nearest degree Fahrenheit.

Two video cameras positioned outside the vacuum tank were used to monitor the test and to study the cathode phenomena. The first camera was perpendicular to the anode axis and was used to observe the thruster plume. The second camera was placed about 20 m away from the thruster looking into the chamber. It was focused on the front end of the cathode at a slight angle to the cathode axis. The cathode camera had a Questar telescope attached to it and was outfitted with proper neutral density filters and narrow band pass (10 nm) filters. The video image was processed using a commercial processing system.

Thruster performance parameters were obtained from a set of panel meters consisting of current, voltage, propellant flow rates, and temperature readouts. The data were also simultaneously fed into a computerized data acquisition system. All instrumentation was calibrated periodically.

MPD THRUSTER AND MAGNET CONFIGURATIONS

A typical thruster, shown schematically in figure 1, consisted of a cylindrical water-cooled anode with a coaxial hollow cathode. A boron nitride backplate was used to electrically insulate the cathode and anode and to inject the propellant through small holes into the discharge chamber. The anode had a radius of 3.8 cm and a length of 7.6 cm.

Four configurations of hollow cathodes, shown in figure 3, were tested. Two types of inserts were used. One consisted of a hollow cylinder, the other had a molybdenum tube brazed to it before the impregnation process. The first two cathode designs were scaled-up versions of ion thruster hollow cathodes, where the insert was press fit into the molybdenum cathode body. This configuration precluded propellant passage to the outside surface of the low work function insert. In the third configuration, the insert was suspended from the cathode end-cap by a threaded 70%Mo30% W alloy support rod. For the fourth configuration, which used the same insert as configuration 3, the outer molybdenum body was cut back 3.5 cm to be even with the BN backplate. This exposed a section of the insert's outer surface to the discharge chamber. The third and fourth cathode configurations permitted propellant flow inside, as well as outside of the insert, though in the fourth configuration the propellant ports to the outside of the insert surface were closed. No attempt was made to insulate the outer cathode body surface in any of the configurations.

Several orifice plates with various orifice sizes were fabricated for each cathode configuration. The orifice plates were simply press fit, not welded, inside the end of the cathode body to expedite the change of orifice plates in the cathode.

The thruster was mounted inside a solenoidal coil which generated the applied magnetic field. Two coil sizes were used. The first had a bore diameter of 15.3 cm and a length of 15.3 cm. It consisted of 36 turns of water-cooled copper tubing. The second had a bore diameter of 20.3 cm and a length of 15.3 cm and contained 28 turns of tubing. The solenoids generated a magnetic axial field strength of 1.66×10^{-4} T/A and 8.48×10^{-5} T/A at the center line of the magnet exit plane for the 15.3 and 20.3 cm magnet, respectively.

Using cathode configurations 1 and 2, the thruster was placed inside the magnet coils such that the anode exit plane was even with the end of the solenoid, with the cathode positioned 2.5 cm from the exit plane of the anode. When cathode configurations 3 and 4 were tested, the exit plane of the anode was located 3.2 cm upstream of the exit plane of the magnet solenoid.

CATHODE HANDLING AND TEST PROCEDURE

Due to the hygroscopic nature of the low work function insert material, it is accepted practice to keep the inserts in hermetically sealed containers while not in use. Before operating a cathode with an insert, it is also usually preheated to remove absorbed water and condition the surface (ref. 22). For these tests, however, special handling of the inserts was not possible during the assembly and testing of the cathodes. In addition, testing with a cathode whose insert had been preheated in an inert atmosphere oven revealed no evident benefits from this procedure, so it was not followed with the other cathodes.

The ignition of the thruster discharge was achieved by presetting a given mass flow rate and magnetic field strength. A set of countdown timers were then activated to turn on the main power supply, send a pulse of gas to the chamber if necessary, and turn on the high voltage igniter in a preset sequence.

The power supplies were set to initiate the discharge at approximately 1000 A. From previous experience with conventional cathodes, this current level was found to result in "smooth" ignition, characterized by relatively little particulate ejection and discharge voltage instability (ref. 23). However, since no previous hollow cathode experience existed at high power levels, starting conditions were occasionally varied to achieve ignition.

In these preliminary tests the temperature and the ambient pressure of the cathode insert were not measured. Such measurements will be required in the future.

RESULTS AND DISCUSSION

The results of initial ignition tests of the four cathode configurations are described first. Performance measurements of the cathode and thruster configurations which operated stably with the discharge attached to the insert are then described, followed by a summary of the implications of these thruster performance measurements for cathode operation, performance, and long term stability.

CATHODE OPERATION

Ignition was achieved with hollow cathodes with configurations 1 and 2 (fig. 3), however, stable discharge current attachment to the insert was not attained for applied fields between 0 and 0.09 T, and propellant flow rates between 0.1 and 0.5 g/sec. Severe particulate ejection was observed once the ignition took place. The press fit orifice plates did not stay in place in either cathode, so the cathodes were tested without them. It was observed from the cathode camera that discharge current attachment was unstable, "jumping" between the insert and the outer body. Very bright spots indicated localized current attachment to the cathode body. The photograph in figure 4 shows the damage to the front of the four cathode bodies. No visible damage was observed on the two inserts. The insert did not disintegrate from the lack of proper "preconditioning." Before the two configurations are ruled out for future use, the cathode configurations should be tested with the orifice plates rigidly attached to the cathode body.

Initial tests with cathode 3 yielded similar results. The discharge apparently attached to the tip of the cathode body resulting in severe particulate ejection. During the second start, the

orifice plate came off and melted on the bottom of the anode. The third start was less eventful as the discharge slowly transferred from the outer body to the insert with the discharge voltage becoming more stable. After about 5 min, the discharge had stabilized on the insert. In subsequent starts the discharge ignited inside the insert.

Successful starts were obtained by presetting the applied magnetic field to 0.04 T, the argon mass flow rate to between 0.15 to 0.2 g/sec, and the initial discharge current to approximately 1000 A.

Even though some damage was suffered by the cathode body during the start-up of the cathode configuration 3, it is believed that the data presented should not be affected by the distorted front end of the cathode body. It is not clear if some damage was suffered by the insert due to possible metal vapor condensation on the insert during the melt down period. There was no apparent current attachment to the cathode body during the ignition and operation of cathode configuration 4.

THRUSTER PERFORMANCE

Typical current-voltage characteristics for cathode configuration 3 are shown in figure 5(a). It is evident that the discharge voltage was strongly affected by both the discharge current and the applied-field (ref. 24). At a discharge current of 1000 A, the discharge voltage increased from 13.5 V at no applied field to 52.1 at an applied-field of 0.124 T, for argon flow rate of 0.14 g/sec. Increasing the magnetic field too high for a given discharge current resulted in the discharge current attachment transferring from the insert to the cathode body.

The discharge voltage was lowest with no applied magnetic field. A conventional thruster operating with the same kind of anode and applied-field could not sustain a stable discharge without the applied-field (ref. 23 and 24). It is not clear if this difference in thruster behavior was due to the lower work function of the hollow cathode or the inherently different current distribution of the two cathodes. The hollow cathode thruster discharge current was limited to approximately 1750 A without an applied-field. Increasing the discharge current lowered the magnitude of the maximum applied-field at which the discharge became unstable. As the discharge current and applied-field were increased above 2000 A and 0.08 T, respectively, loss of copper from the anode became evident. The curve with three data points 3 V above the 0.083 T curve in figure 5(a) correspond to discharge current attachment to the cathode body and designated as the high voltage mode. This voltage difference between the two modes was considerably larger at lower discharge current levels.

Figure 5(b) shows the current-voltage characteristics for an applied-field of 0.033 T at argon mass flow rates of 0.08, 0.10, and 0.14 g/sec. The discharge voltage increased with decreasing propellant flow rate. At lower mass flow rates, a sudden decrease of the discharge voltage was observed at discharge current levels below approximately 750 A. The discharge current of 2250 A represents the highest current attained during these tests. Relative brightness profiles indicated that both the insert and the cathode body were very hot and probably indicated current attachment to both parts of the hollow cathode at high discharge current and applied-field levels.

The transition of the current attachment from the insert to the cathode outer body with increasing applied field is shown in figure 6, where the brightness profile across the cathode face

is plotted. These data were obtained using the cathode camera and the video image processing system. At an applied-field of 0.033T, the highest temperature (intensity) was seen on the inside edge of the insert. As the applied field was increased to 0.051 T, the whole insert, as well as the cathode outer body temperature, became hotter. The current attachment transitioned totally to the outer body at applied-field of 0.059T is observed in figure 6(b). The cathode body became extremely hot as the insert cooled down.

Eventual failures of the thruster, however, were due to pinhole water leaks on the cathode rim of the anode at high power levels. Arc attachment spots, as indicated by highly luminous regions, were observed on the lip of the anode just before the water leak. Some melting of the front end of the cathode body can be seen in figure 4. This melting was assumed to have taken place during the discharge attachment to the cathode body at the beginning of the tests.

Thrust efficiency of cathode configuration 3 as a function of specific impulse is shown in figure 7. The highest specific impulse, 2010 sec, with thrust efficiency of close to 18 percent, was attained at a discharge current of 1000 A, an applied field strength of 0.083 T, and an argon flow rate of 0.08 g/sec. A specific impulse of 1950 sec at an efficiency of 5.5 percent was attained with no applied field and a propellant mass flow rate of 0.022 g/sec. A maximum power of 115 kW was reached.

The performance of hollow cathode configuration 4 was considerably lower than that of configuration 3. The highest specific impulse and thrust efficiency obtained were 1370 s, and 11.0 percent respectively, at a discharge current of 1000 A, applied field of 0.017 T, and argon mass flow rate of 0.061 g/sec. The performance of configuration 4 may have been limited by plasma leakage through the 0.12 cm propellant holes in the BN backplate. Bright spots appeared in these holes on the backplate as the applied field was increased beyond 0.03 T. Decreasing the size of the propellant injection ports by a factor of two did not seem to help the problem.

Figure 8 shows the specific impulse plotted as a function of the applied-field strength for hollow cathode configuration number 3 and for a conventional rod-shaped cathode. The rod-shaped 2 percent ThO_2 tungsten cathode was 1.27 cm in diameter. The data were obtained at a discharge current of 1000 A and an argon mass flow rate of 0.14 g/sec. The specific impulse increased monotonically with the applied-field strength. Hollow cathode configuration 3 yielded about the same specific impulse as a conventional MPD thruster at lower applied fields from 0.04 to 0.06 T (ref. 24).

CATHODE PERFORMANCE

The principal advantage of a hollow cathode, if operated in the proper thermal environment, appears to be its ability to retain the low work function material on the cathode without restricting the discharge chamber design options. Ideally, the cathode should operate at a temperature and pressure for which the loss rate of barium at the surface of the insert is equal to the diffusion rate of the barium atoms to the insert surface. The insert should not operate at temperatures at which chemical reactions take place with the barium. These reactions can increase the cathode work function, resulting in a higher operating temperature. Because the cathode temperature was not monitored, it was difficult to assess the insert condition after more than the 20 hr of accumulated run time. The impact of these potential problems, therefore, must be assessed from the time dependence of the thruster performance parameters.

A change in the cathode characteristics may be manifested in the performance of the thruster in several ways. While the complexity of applied-field MPD thrusters precludes definitive statements without more detailed measurements, a dramatic change in the cathode work function would most likely result in a change in the cathode fall voltage, which in turn would increase the discharge voltage. These changes should, therefore, be manifested in changes in the temporal behavior of the discharge current - voltage characteristics. Discharge voltage characteristics of cathode configuration 3 without an applied magnetic field are shown in figure 9. The lowest discharge voltages were measured during the first test after about 1.5 hr of thruster operation. The discharge voltage at discharge current of 500 A was only 11.4 V and increased to 17.6 V at a discharge current of 1500 A. These voltages rose during the third test after approximately 6 hr of total test time. The voltage increased by 2.4 V at a discharge current of 500 A, and by 4 to 7 V at discharge currents of 1000 to 1500 A. The reason for this increase is not clear, though it may be associated with an increased work function, a change in emission mode, or be the result of cathode contamination during the anode failure ending the first run of this cathode configuration. When the discharge voltage-current curve was taken after about 2 hr into the next test, or after about 76 had almost returned to its initial condition. However, the voltage was approximately 2.0 V higher than the initial test. Plotted another way, figure 10 shows the discharge voltage as a function of time. Thrust values for each operating condition are given next to each data point. The thruster appeared to operate normally for about the first 4 hr of testing. At this point, an increase in voltage was observed, correlated with a small increase in thrust. The decrease in discharge voltage observed during the last 2 hr of testing is clearly evident in figure 10. Thus, the net change in voltage which occurred over the course of 10 hr of testing was only 2 V, indicating that while the cathode may have suffered some degradation, the changes do not appear to be dramatic.

CONCLUSION

Four hollow cathode configurations with low work function inserts were tested in a steady-state 100 kW class applied field MPD thruster. Two of the configurations exhibited stable discharge current attachment to the insert of the hollow cathode. For these two MPD thruster configurations the performance was mapped over a range of argon mass flow rates (0.22 to 0.15 g/sec), applied magnetic field strengths (0 to 0.125 T), and discharge currents (500 to 2000 A). The performance of the first successful configuration compared favorably to a conventional cathode rod MPD thruster. Thrust efficiencies of close to 20 percent were attained with specific impulse of up to 2000 sec. The second successful configuration did not perform as well as the first configuration. Discharge current leakage back through the propellant port holes may have contributed to the low performance of the second cathode.

Over a 10 hr run time, the discharge voltage increased by approximately 10 percent, indicating some degradation of the cathode. The discharge attachment was observed to transition from the insert to the cathode outer body if the applied magnetic field was too strong. The attachment of the discharge to the cathode body is certainly undesirable. Even though some melting of the front cathode was observed, it is believed that the data presented here was not unduly affected by it.

These tests showed that a hollow cathode with a low work function insert was capable of operating over a range of MPD thruster parameters. While several problems were identified, it appears that hollow cathodes have the potential for eliminating the principal MPD thruster life

limiter. Future work should focus on measurements of the cathode surface temperature and the internal cathode pressure.

ACKNOWLEDGEMENTS

The authors would like to thank Elmer Petelka for his skill in fabricating the hollow cathodes, John Naglowsky, Larry Schultz, John Eckert, Tom Ralys, David Wolford, John McAlea, Rob Butler, John Miller, Gerry Schneider, and Cliff Schroeder for their assistance in preparing and maintaining the experimental apparatus, and Inara Punga for her dedicated help in the preparation of this paper.

REFERENCES

1. Sovey, J.S. and Mantenieks, M.A., "Performance and Lifetime Assessment of Magnetoplasma-dynamic Arc Thruster Technology," Journal of Propulsion and Power, Vol. 7, No. 1, Jan-Feb. 1991, pp. 71-83.
2. Myers, R.M., Mantenieks, M.A., and LaPointe, M.R., "MPD Thruster Technology," AIAA Paper 91-3568, Sept. 1991.
3. Polk, J.E., Kelly, A.J., and Jahn, R.G., Kurtz, M.L.; and Auweter-Kurtz, M., "Mechanisms of Hot Cathode Erosion in Plasma Thrusters," AIAA Paper 90-2673, July 1990.
4. Myers, R.M., Suzuki, N., Kelly, A.J., and Jahn, R.G., "Cathode Phenomena in a Low Power, Steady State MPD Thruster," AIAA Paper 88-3206, July 1988; see also Journal of Propulsion and Power, Vol. 7, No. 5, Sept-Oct. 1991, pp. 760-766.
5. Auweter-Kurtz, M., Glocker, B., Kurtz, H.L., Loesener, O., Schrade, H.O., and Tubanos, N., "Cathode Phenomena in Plasma Thrusters," AIAA Paper 90-2662, July 1990.
6. Kristiansen, M., and Hatfield, L., Workshop Co-Chairmen, "Electrode Erosion in Electric Space Propulsion Engines," Texas Tech Univ., Lubbock, TX, May 1989, p. 162.
7. Meunier, J.L. and Drouet, M.G., "Experimental Study of the Effect of Gas Pressure on Arc Cathode Erosion and Redeposition in He, Ar, and SF(6) from Vacuum to Atmospheric Pressure," IEEE Transactions on Plasma Science, Vol. PS-15, No. 5, Oct. 1987, pp. 515-519.
8. Auweter-Kurtz, M., and Messerschmid, E., "Plasma Accelerator Activities at the IRS," AIAA Paper 90-2659, July 1990.
9. Mirtich, M.J. and Kerslake, W.R., "Long Lifetime Hollow Cathodes for 30-cm Mercury Ion Thrusters," AIAA Paper 76-985, Nov. 1976. (Also, NASA TM X-73523).
10. Yoshikawa, T., Kagaya, Y., Tahara, H., and Wasa, T., "Continuous Operation of a Quasi-Steady MPD Thruster Propulsion System with an External Magnetic Field," 20th International Electric Propulsion Conference, DGLR, Bonn, West Germany, 1988, pp. 315-322.

11. Goebel, D.M., Hirooka, Y., and Sketchley, T.A., "Large-Area Lanthanum Hexaboride Electron Emitter," Rev. Sci. Instruments, Vol. 56, No. 9, Sept. 1985, pp. 1717-1722.
12. Collett, C., "Thruster Endurance Test," NASA CR-135011, 1976.
13. Mantenicks, M.A., "Hg Ion Thruster Component Testing," AIAA Paper 79-2116, Oct. 1979, (also, NA3A TM-79287, unpublished data of the author).
14. Wilbur, P.J., "Advanced Electric Propulsion and Space Plasma Contactor Research," NASA CR-180862, 1987.
15. Toki, K., "Quasisteady MPD Arcjet with Hollow Cathode," Journal of Propulsion and Power, Vol. 2, No. 5, Sept.- Oct. 1986, pp. 402-407.
16. Toki, K., and Kimura, I., "Studies of Current Distribution on the Hollow Cathode of an MPD Arcjet," AIAA Paper 79-2113, Nov. 1979.
17. Krishnan, M., Jahn, R.G., Von Jaskowsky, W.F., and Clark, K.E., "Physical Processes in Hollow Cathodes," AIAA Journal, Vol. 15, No. 9, Sept. 1977, pp. 1217-1223.
18. Parmentier, N., and John, R.G., "Hollow Cathode, Quasi-Steady MPD Arc," REPT-1023, Princeton University, NASA- CR-127749, Dec. 1971.
19. Sovey, J.S., Mantenicks, M.A., Haag, T.W., Raitano, P., and Parkes, J.S., "Test Facility and Preliminary Performance of a 100 kw Class MPD Thruster, NASA TM-102021, 1989.
20. Mantenicks, M.A., Sovey, J.S., Myers, R.M., Raitano, P., and Parkes, J.E., "Performance of a 100 kW Class Applied Field MPD Thrusters," AIAA Paper 89-2710, July 1989, (also, NASA TM-102312).
21. Haag, T.W., "Thrust Stand for High-Power Electric Propulsion Devices," Rev. Sci. Instrum., Vol. 62, No. 5, May 1991, pp. 1186-1191 (also, NASA-TM 102372).
22. Verhey, T.R., and MacRae, G.S., "Requirements for Long-Life Operation of Inert Gas Hollow Cathodes-Preliminary Results," AIAA Paper 90-2586, July 1990 (also, NASA TM-103242).
23. Myers, R.M., Mantenicks, M.A., and Sovey, J., "Geometric Effects in Applied-Field MPD Thrusters," AIAA Paper 90-2669, July 1990 (also, NASA TM-103259).
24. Myers, R.M., "Applied-Field MPD Thruster Geometry Effects," AIAA Paper 91-2342 June 1991 (also, NASA CR-187163).

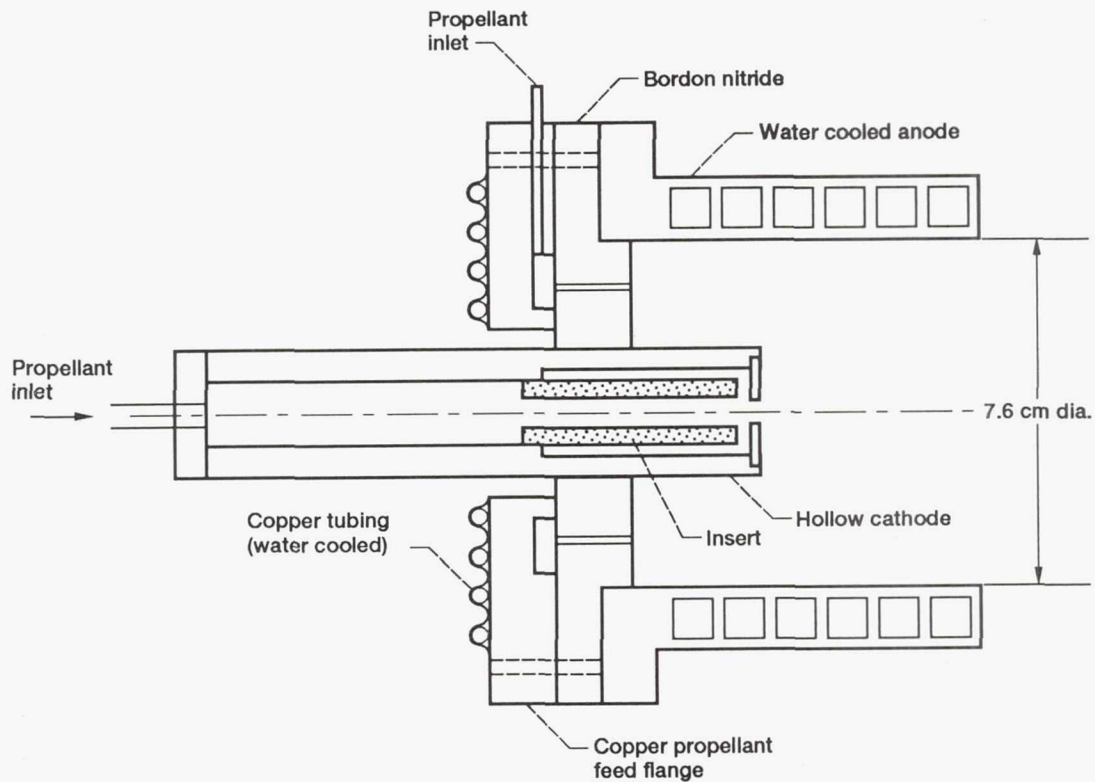


Figure 1.—Schematic of hollow cathode MPD thruster.

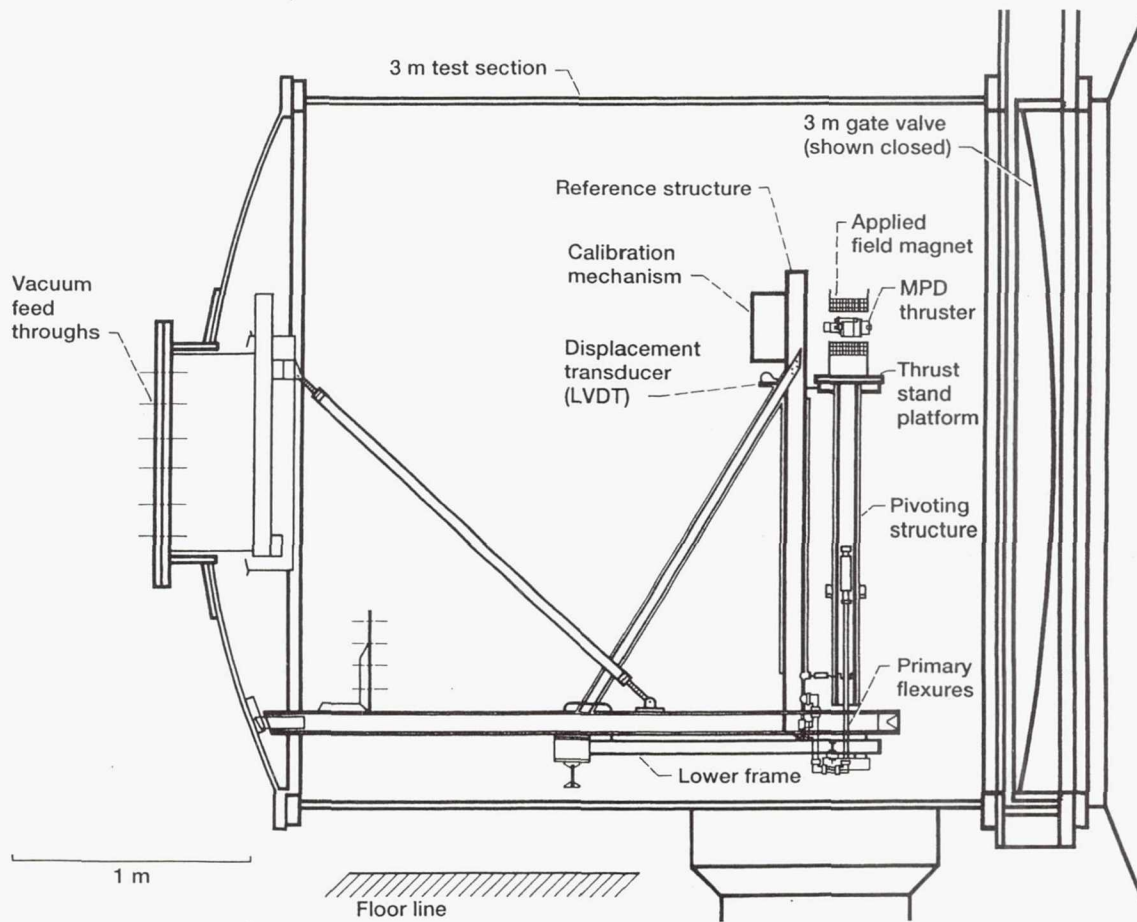


Figure 2.—Schematic of MPD thruster with thrust stand.

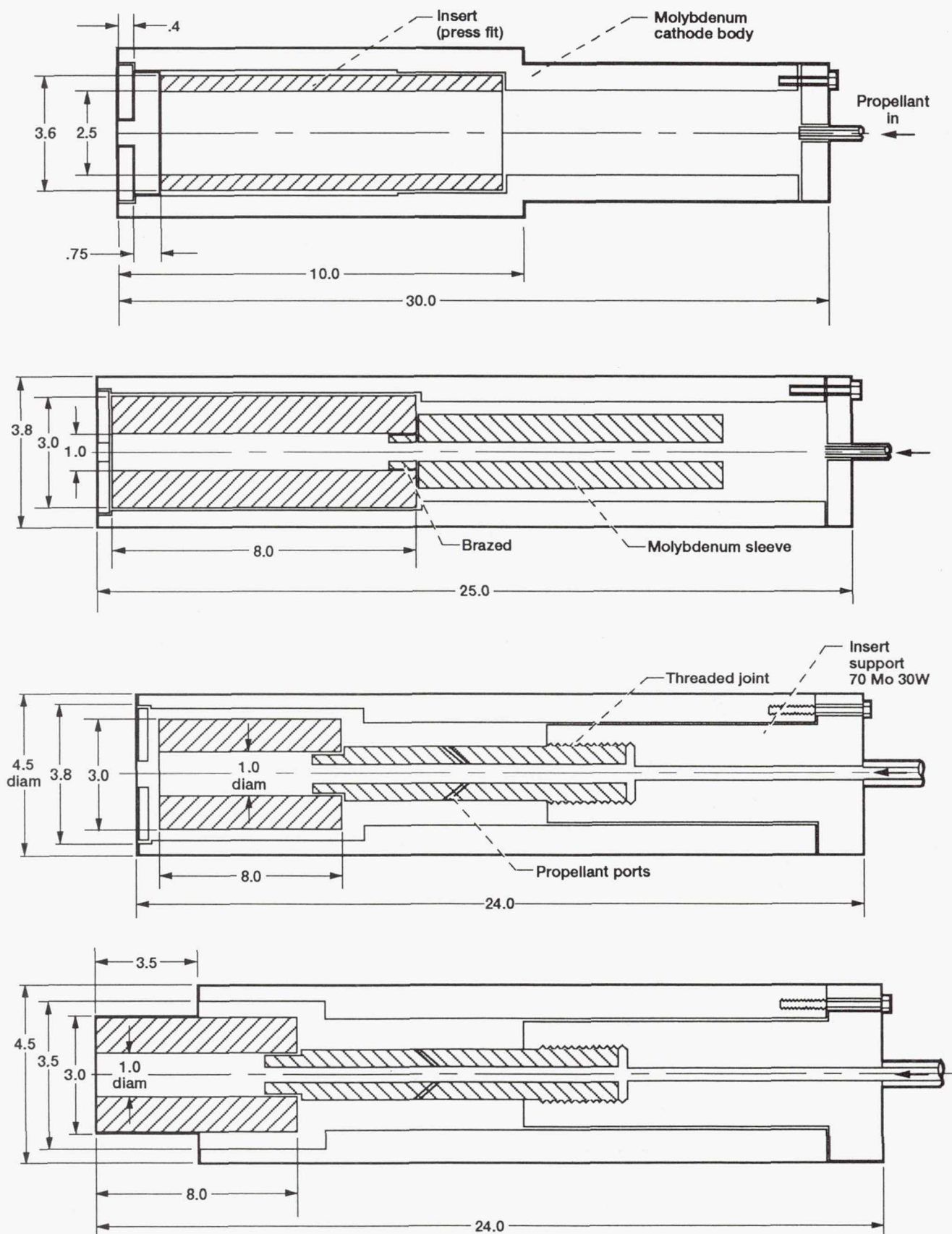


Figure 3.—Hollow cathode configurations. (Dimensions in cm. Not to scale.)



C-91-09099

Figure 4.—Hollow cathode configurations after tests: from the left - #1, #2, #3 (without insert), and #4.

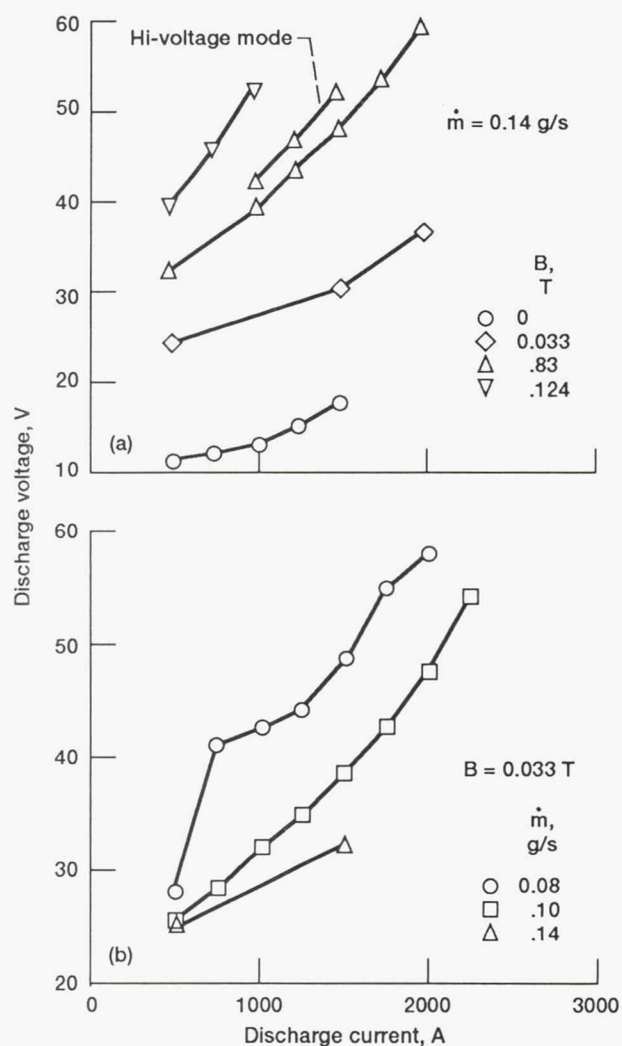


Figure 5.—Discharge voltage-current (JD) characteristics with hollow cathode configuration #3 at various: (a) applied-field strengths (B) and (b) mass flow rates (\dot{m}).

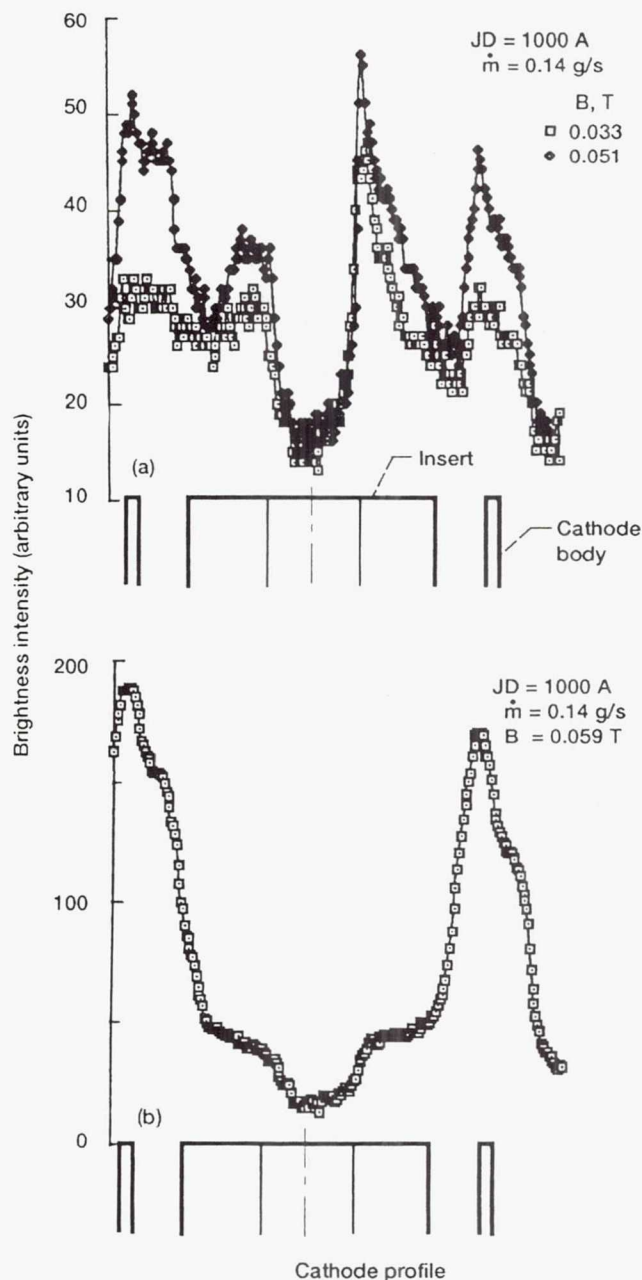


Figure 6.—Brightness intensity profiles across the hollow cathode showing region of intense current attachment. Applied field strengths of 0.033, 0.051 T (a) and 0.059 T (b).

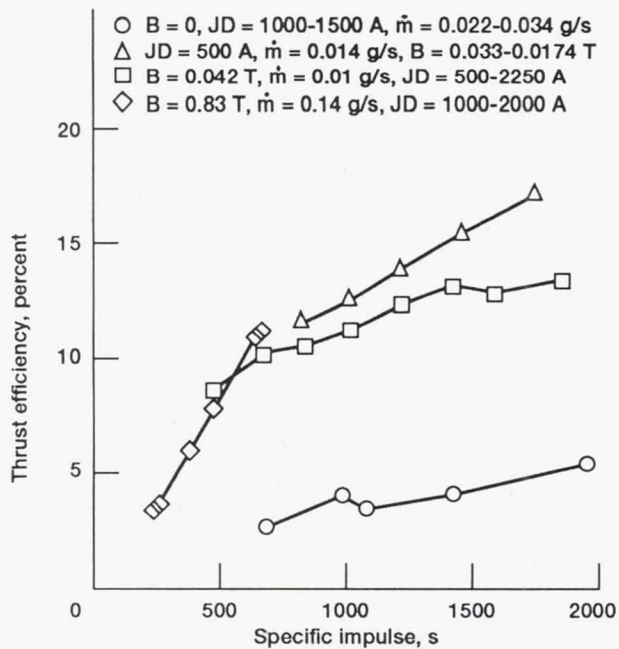


Figure 7.—Efficiency as a function of specific impulse for hollow cathode configuration #3.

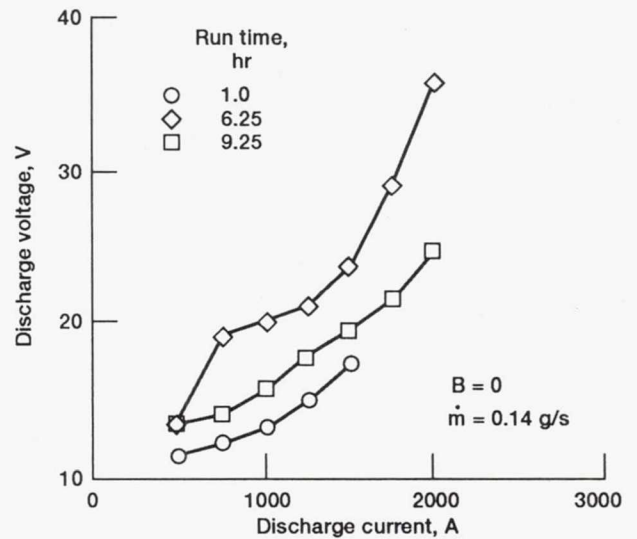


Figure 9.—Discharge current-voltage characteristics at various times for hollow cathode configuration #3.

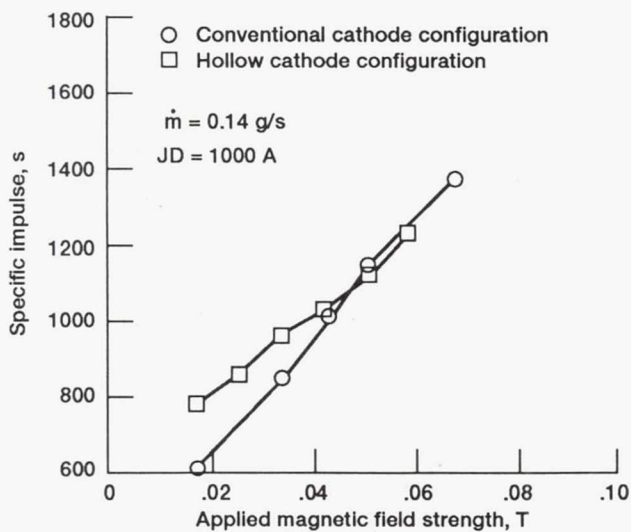


Figure 8.—Specific impulse as a function of applied field strength for hollow cathode configuration #3 and conventional rod cathode.

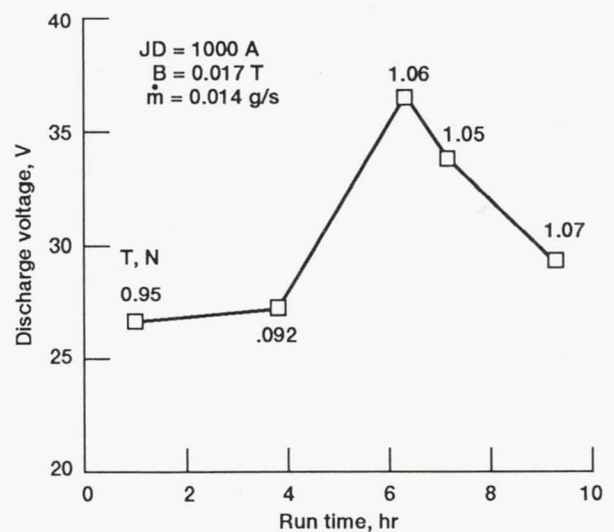


Figure 10.—Discharge voltage at various times for hollow cathode configuration #3. (Numbers by data points denote thrust levels).

REPORT DOCUMENTATION PAGE			Form Approved OMB No. 0704-0188	
Public reporting burden for this collection of information is estimated to average 1 hour per response, including the time for reviewing instructions, searching existing data sources, gathering and maintaining the data needed, and completing and reviewing the collection of information. Send comments regarding this burden estimate or any other aspect of this collection of information, including suggestions for reducing this burden, to Washington Headquarters Services, Directorate for Information Operations and Reports, 1215 Jefferson Davis Highway, Suite 1204, Arlington, VA 22202-4302, and to the Office of Management and Budget, Paperwork Reduction Project (0704-0188), Washington, DC 20503.				
1. AGENCY USE ONLY (Leave blank)	2. REPORT DATE 1991	3. REPORT TYPE AND DATES COVERED Technical Memorandum		
4. TITLE AND SUBTITLE Preliminary Test Results of a Hollow Cathode MPD Thruster		5. FUNDING NUMBERS WU-506-42-31		
6. AUTHOR(S) Maris A. Mantenicks and Roger M. Myers				
7. PERFORMING ORGANIZATION NAME(S) AND ADDRESS(ES) National Aeronautics and Space Administration Lewis Research Center Cleveland, Ohio 44135-3191		8. PERFORMING ORGANIZATION REPORT NUMBER E-6608		
9. SPONSORING/MONITORING AGENCY NAMES(S) AND ADDRESS(ES) National Aeronautics and Space Administration Washington, D.C. 20546-0001		10. SPONSORING/MONITORING AGENCY REPORT NUMBER NASA TM-105324 IEPC-91-076		
11. SUPPLEMENTARY NOTES Prepared for the 22nd International Electric Propulsion Conference cosponsored by AIDAA, AIAA, DGLR, and JSASS, Viareggio, Italy, October 14-17, 1991. Maris A. Mantenicks, NASA Lewis Research Center; Roger M. Myers, Sverdrup Technology, Inc., Lewis Research Center Group, 2001 Aerospace Parkway, Brook Park, Ohio 44142. Responsible person, Maris A. Mantenicks, (216) 977-7460.				
12a. DISTRIBUTION/AVAILABILITY STATEMENT Unclassified - Unlimited Subject Category 20		12b. DISTRIBUTION CODE		
13. ABSTRACT (Maximum 200 words) Performance of four hollow cathode configurations with low work function inserts has been evaluated in a steady-state 100 kW class applied magnetic field MPD thruster. Two of the configurations exhibited stable discharge current attachment to the low work function inserts of the hollow cathodes. A maximum discharge current of 2250 A was attained. While the applied-field increased the performance of the thruster, at high applied-fields the discharge current attachment moved from the insert to the cathode body. The first successful hollow cathode performed well in comparison with a conventional rod cathode MPD thruster, attaining a thrust efficiency with argon of close to 20 percent at a specific impulse of about 2000 s. The second successful configuration had significantly lower performance.				
14. SUBJECT TERMS Electric propulsion; Space propulsion; MPD thruster			15. NUMBER OF PAGES 16	
			16. PRICE CODE A03	
17. SECURITY CLASSIFICATION OF REPORT Unclassified	18. SECURITY CLASSIFICATION OF THIS PAGE Unclassified	19. SECURITY CLASSIFICATION OF ABSTRACT Unclassified	20. LIMITATION OF ABSTRACT	